Supporting Information

Reconstruction of AgPd Nanoalloy with Oxidation for Formate Oxidation Electrocatalysis†

Longfei Guo, [a,b] *Tao Jin,* [a] *Quan Tang,* [b] *Junpeng Wang,* [a] *Bowei Pan,* [a] *Qiao Wang,* [a] *Zhen Li,* [b] *Chongyang Wang,* [b] *Jiawang Liu,* [b] *Fuyi Chen.** [a,b]

a State Key Laboratory of Solidification Processing, Northwestern Polytechnical University, Xi'an 710072, China

b School of Materials Science and Engineering, Northwestern Polytechnical University, Xi'an, 710072, China

*Corresponding author: E-mail: fuyichen@nwpu.edu.cn

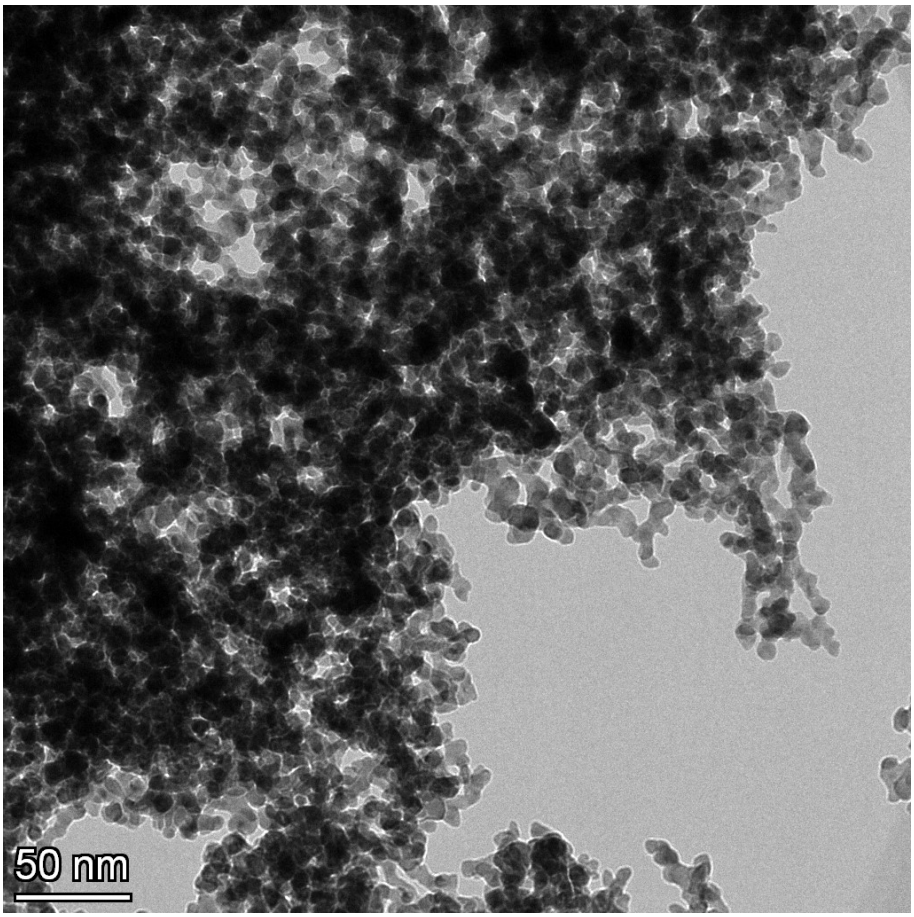

Fig. S1 TEM Bright field image of as-prepared AgPd aerogel.

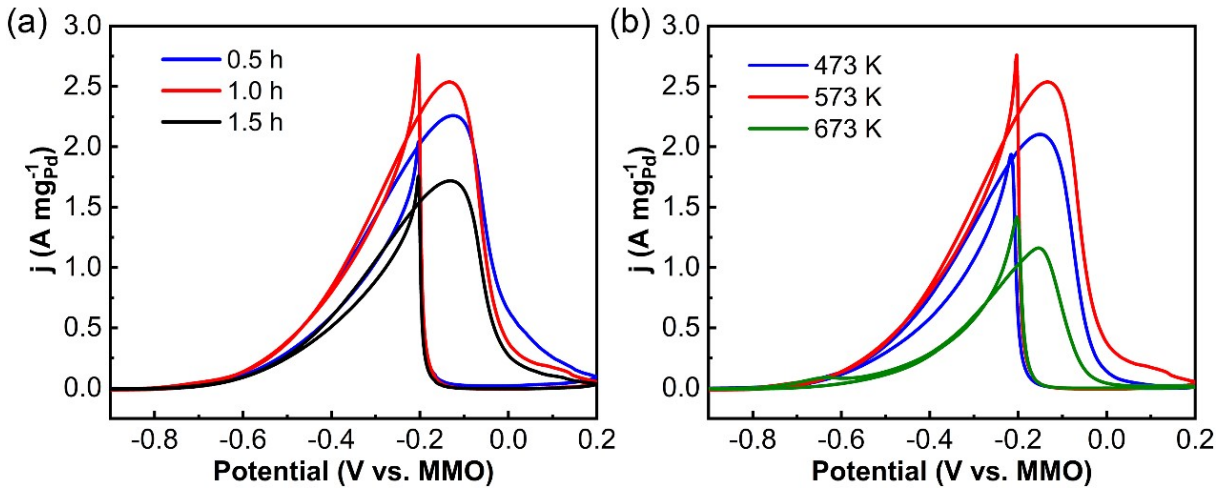

Fig. S2 CV curves of AgPd nanoalloys treated with different (a) time and (b) temperature during oxidation. The electrolyte is 1.0 M KOH +1.0 M HCOOK and the scan rate is 50 mV s^{-1}.

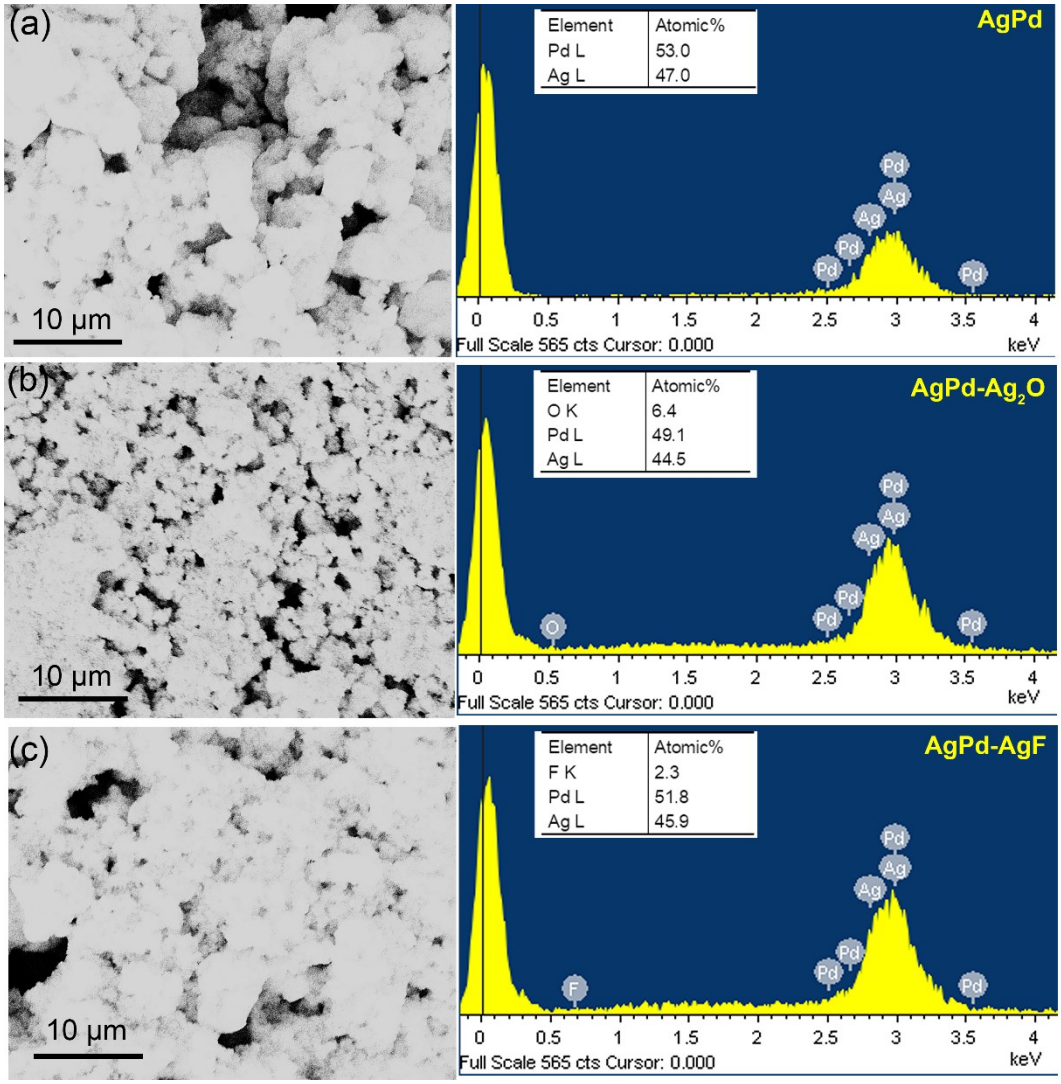

Fig. S3 SEM-EDS for (a) AgPd, (b) AgPd-Ag_2O and (c) AgPd-AgF interfaces, the inset shows the atomic fractions for the elements.

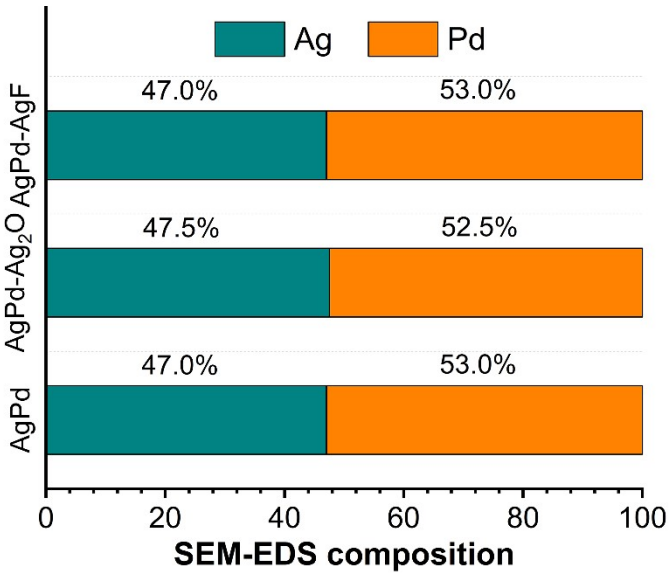

Fig. S4 The relative percentages of Ag/Pd for AgPd, AgPd-Ag_2O and AgPd-AgF interfaces.

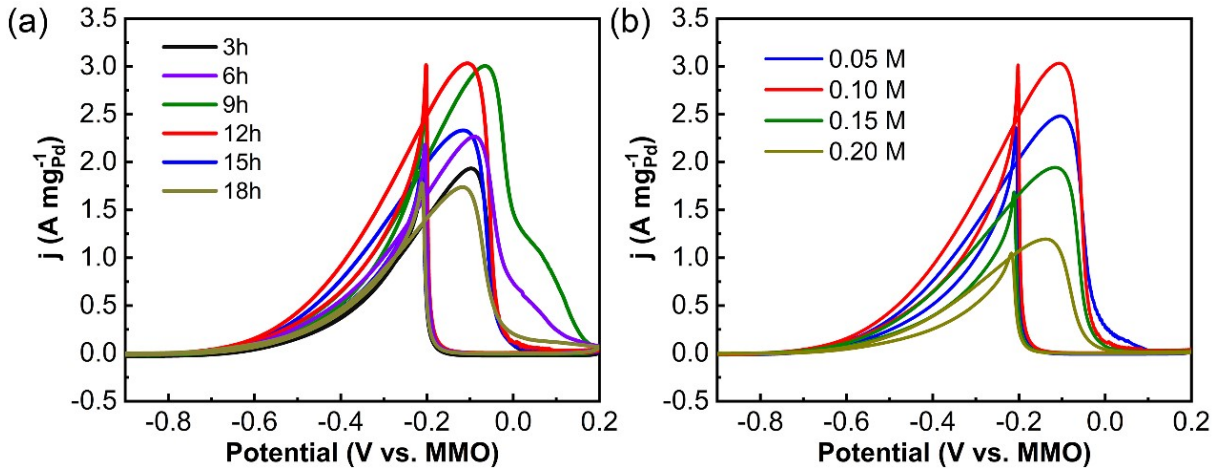

Fig. S5 CV curves of AgPd nanoalloys treated with different (a) time and (b) concentration of ammonium fluoride solution during fluorination at 373K. The electrolyte is 1.0 M KOH +1.0 M HCOOK and the scan rate is 50 mV s^{-1}.

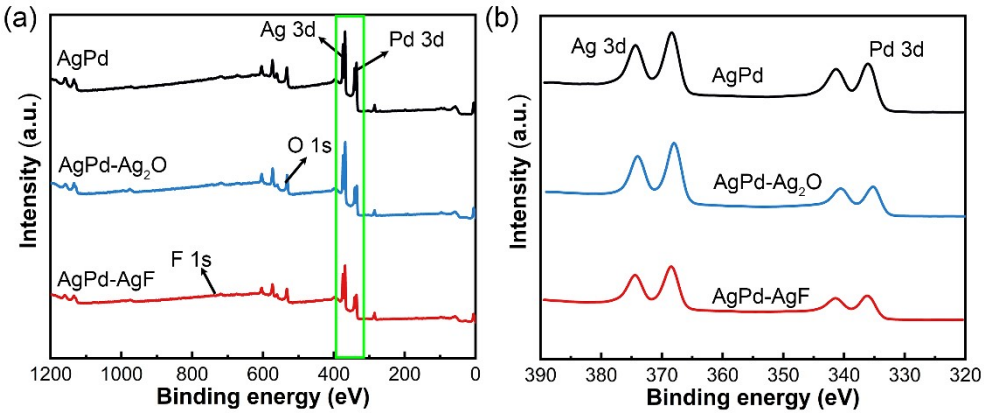

Fig. S6 (a) XPS wide spectrum of AgPd-Ag_2O and AgPd-AgF interfaces with refer to as-prepared AgPd surface. (b) Enlarged spectrum of the green region in (a).

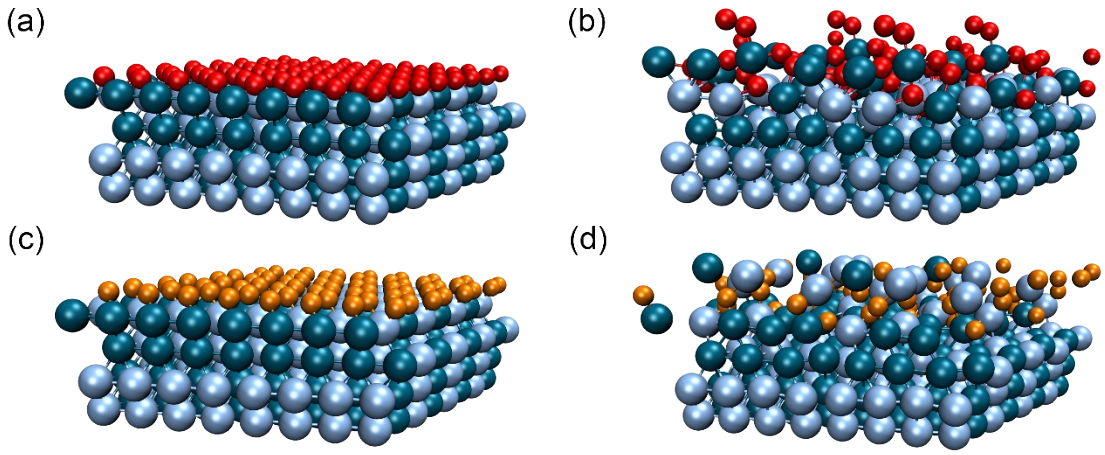

Fig. S7 Ab initio molecular dynamics (AIMD) simulations of oxidation and fluorination process on AgPd(111) surface. (a, c) DFT relaxed structure of AgPd(111) surface with oxygen and fluorine atoms coverage of 1.0 ML. (b, d) Surface structures after 5 ps relaxation of AIMD at 700 K for (a) and (c). The color of light-blue, dark-blue, red and orange are represent for Ag, Pd, O and F atoms.

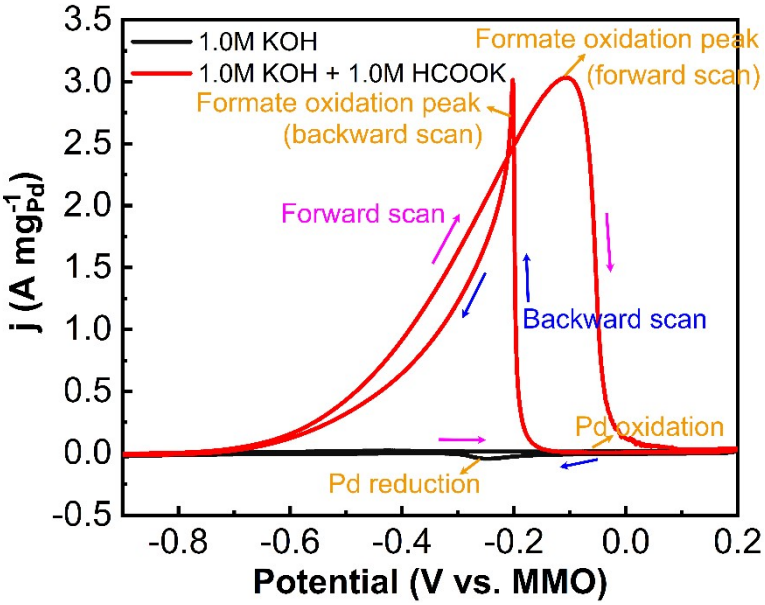

Fig. S8 CV curves of AgPd-AgF interface in electrolyte of 1.0 M KOH and 1.0 M KOH + 1.0 M HCOOK, where the scan rate is 50 mV s^{-1}, the pink and blue arrows indicate the scan direction.

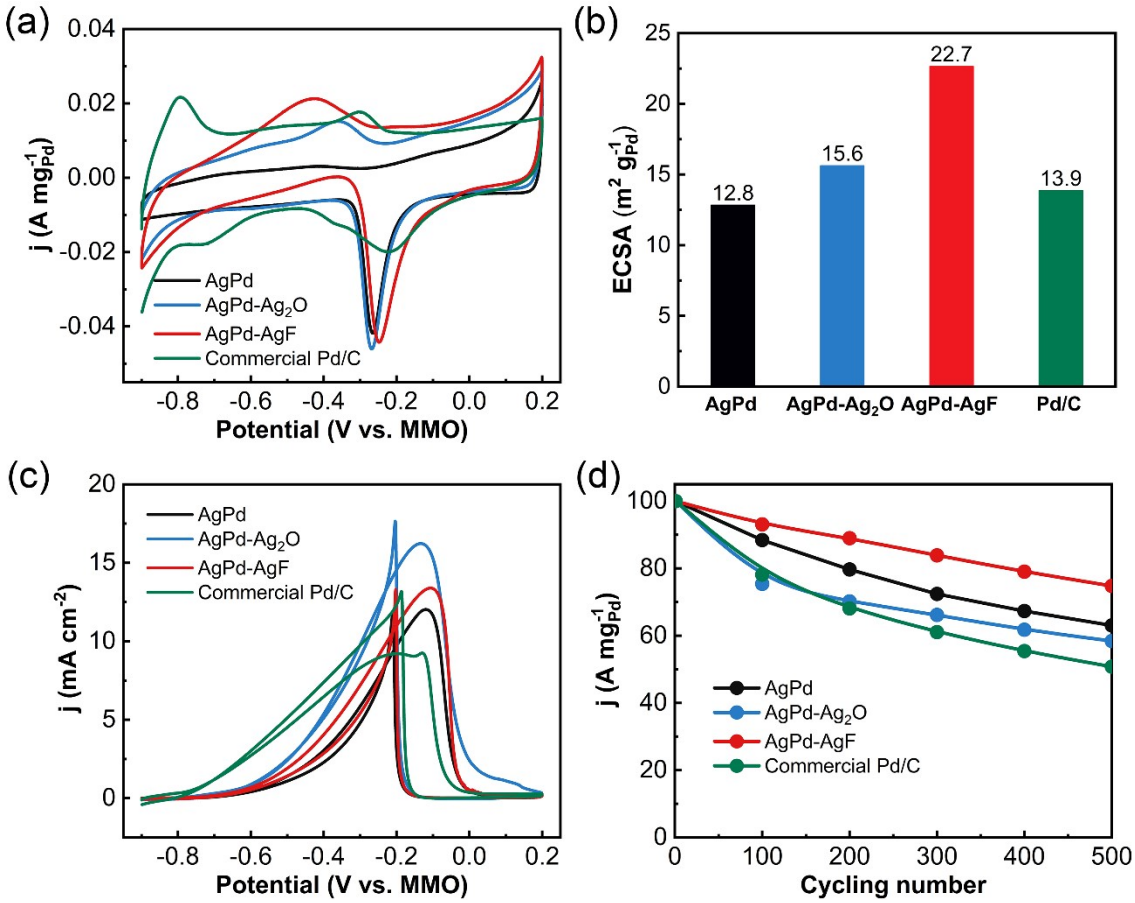

Fig. S9 (a) CV curves and (b) ECSAs of AgPd-Ag_2O and AgPd-AgF interfaces with refer to as-prepared AgPd and commercial Pd/C catalysts. (c) CV curves modified by ECSAs. (d) Cycling stability of AgPd-Ag_2O and AgPd-AgF interfaces with refer to as-prepared AgPd and commercial Pd/C catalysts.

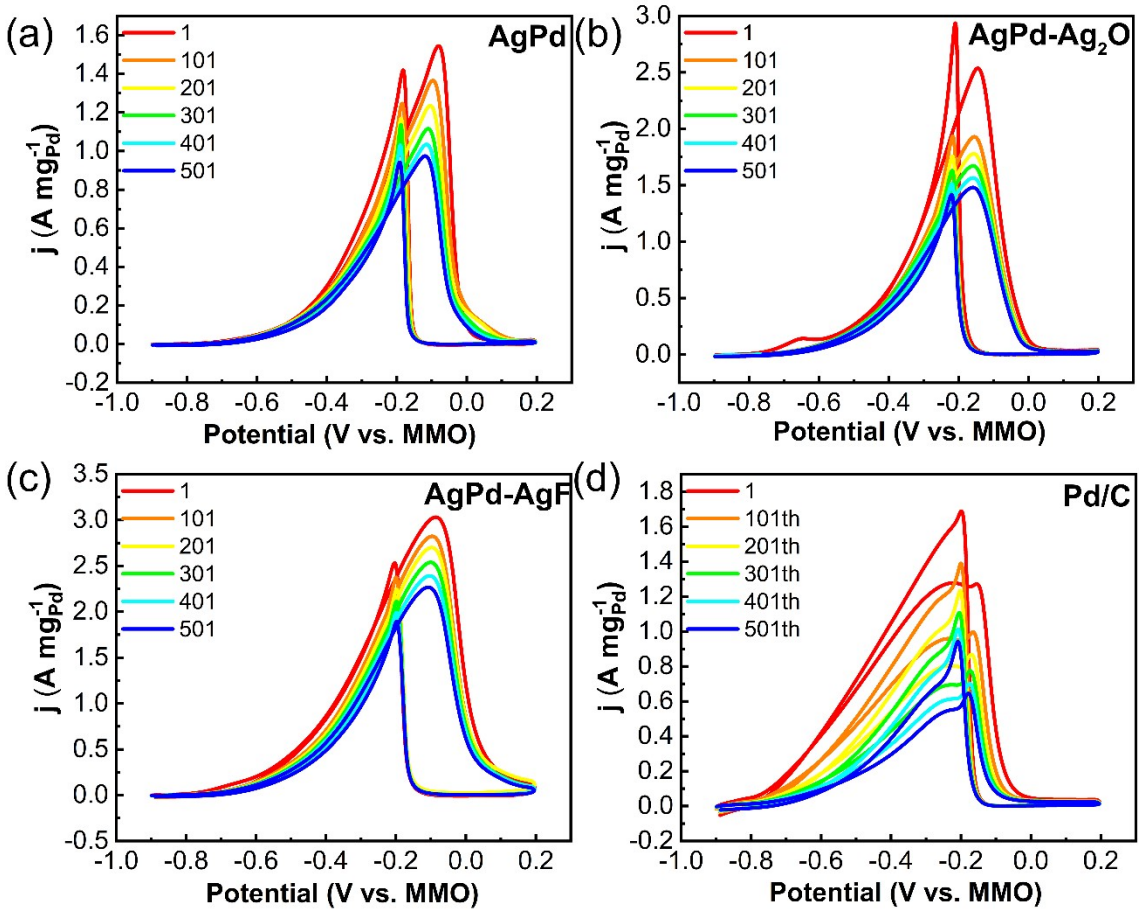

Fig. S10 Cycling stability of AgPd-Ag_2O and AgPd-AgF interfaces with refer to as-prepared AgPd and commercial Pd/C catalysts.

Table S1. A literature survey of the catalytic activity and stability of Ag-based and Pd-based FOR catalysts.

Catalysts	Mass activity (A mg^{-1})	Specific activity (mA cm^{-2})	Scan rete (mV s^{-1})	Stability (after CA)	Cycling stability	Electrolyte	Ref.
AgPd-AgF	**3.03**	**13.38**	**50**	**59.37% (0.968 A mg^{-1}) after 1h**	**74.8% after 500 cycles**	**1.0 M KOH+1.0 M HCOOK**	**This work**
AgPd-Ag_2O	**2.54**	**16.23**	**50**	**28.21% (0.456 A mg^{-1}) after 1h**	**58.4% after 500 cycles**	**1.0 M KOH+1.0 M HCOOK**	**This work**
$Pd_{2.3}Co$/C	2.5	NA	50	0.156 A mg^{-1} after 3000s	NA	1.0 M KOH+1.0 M HCOOK	[1]
PdH/C	NA	0.1	20	31.67% after 1000s	NA	1.0 M KOH + 0.1 M HCOOK	[2]
Pd_4Ag/C	0.04	NA	50	NA	NA	1.0 M NaOH + 0.1 M HCOONa	[3]
PdCu/C	NA	3.5	30	0.182 mA cm^{-2} after 0.5h	NA	1.0 M KOH+1.0 M HCOOK	[4]
CuPdAu/C	1.2	NA	50	0.355 A mg^{-1} after 1000s	NA	0.5 M KOH+0.5 M HCOOK	[5]
PdNi/C	4.5	12.0	50	NA	NA	1.0 M KOH+1.0 M HCOOK	[6]
PdRh/C	4.5	8.1	50	0.408 A mg^{-1} after 6000s	NA	1.0 M KOH+1.0 M HCOOK	[7]
$Pd_{72}Ce_{28}$/C	1.1	19.4	50	NA	11% after 500 cycles	1.0 M KOH+1.0 M HCOOK	[8]
$Ag_{49}Pd_{51}$/rGO	4.2	4.1	50	0.118 A mg^{-1} after 1h	49.1% after 500 cycles	1.0 M KOH+1.0 M HCOOK	[9]
PdAu/Ni foam	NA	0.8	50	NA	NA	0.5 M NaOH + 0.1M HCOONa	[10]
AgCuPd	2.7	10.1	50	NA	38.2% after 500 cycles	1.0 M KOH+1.0 M HCOOK	[11]
$Pd_3Au_3Ag_1$/CNT	4.5	14.3	50	29.3% after 1h	30% after 500 cycles	1.0 M KOH+1.0 M HCOOK	[12]
AgPdF	2.3	20.5	50	0.19 A mg^{-1} after 1h	54% after 600 cycles	1.0 M KOH+1.0 M HCOOK	[13]

$Pd_{55}Ag_{30}Rh_{15}$/C	1.9	3.0	50	0.15 A mg^{-1} after 1h	74.2% after 1000 cycles	1.0 M KOH + 1.0 M HCOOK	[14]
$Pd_6Ag_3Ru_1$/pCNTs	4.7	NA	50	0.7 A mg^{-1} after 5400s	NA	1.0 M KOH + 1.0 M HCOOK	[15]
PdAgIr NFs/C	4.4	6.5	50	27.3% after 4000s	41.5% after 500 cycles	1.0 M KOH + 1.0 M HCOOK	[16]
AgPdPt	2.9	3.5	50	NA	96% after 500 cycles	0.5 M KOH+0.5 M HCOOK	[17]
$Ag_{30}Pd_{69}Co_1$ H-NSs	3.08	16.9	50	0.24 A·mg^{-1} after 1h	54.06% after 500 cycles	1.0 M KOH + 1.0 M HCOOK	[18]
janus-$Ag_{20}Pd_{60}Ni_{20}$	1.3	7.4	50	NA	44.29% after 500 cycles	1.0 M KOH + 1.0 M HCOOK	[19]
Pt-Ag	0.83	NA	50	36% after 10000s	NA	1.0 M KOH + 1.0 M HCOOK	[20]
$Pd_{90}Sn_{10}$/C	5.7	13.5	50	NA	NA	1.0 M KOH + 1.0 M HCOOK	[21]
AgNi@PANI/Pt	0.15	NA	50	0.105 mA cm^{-2} after 1200s	NA	0.2 M H_2SO_4 + 2.0 M HCOONa	[22]

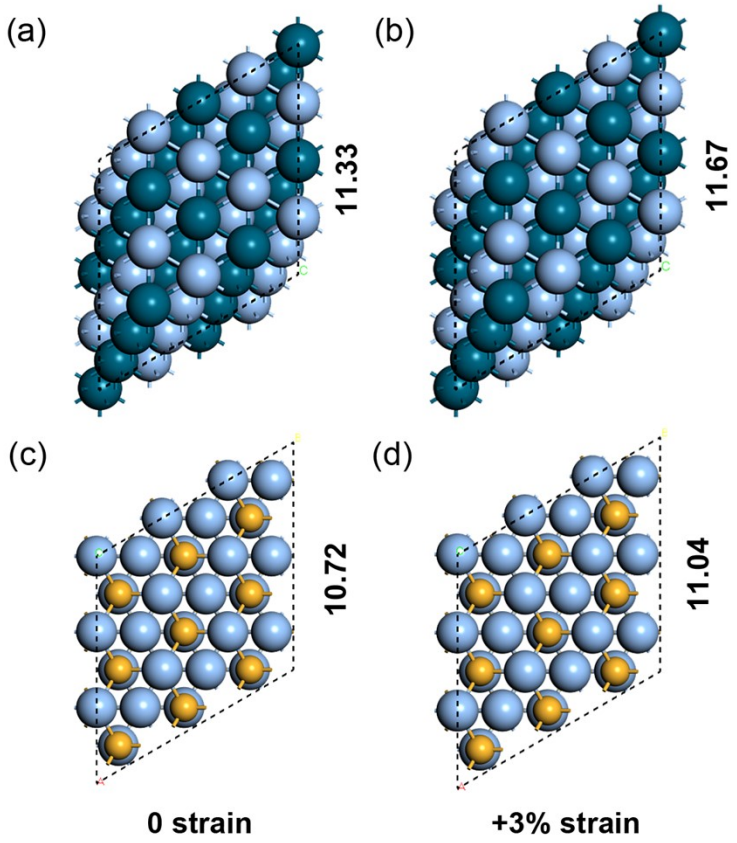

Fig. S11 (a, b) AgPd and (c, d) AgF(111) surfaces with the strain state of 0 and +3%, where the dark blue, light blue and orange are represent for Pd, Ag and F atoms, respectively.

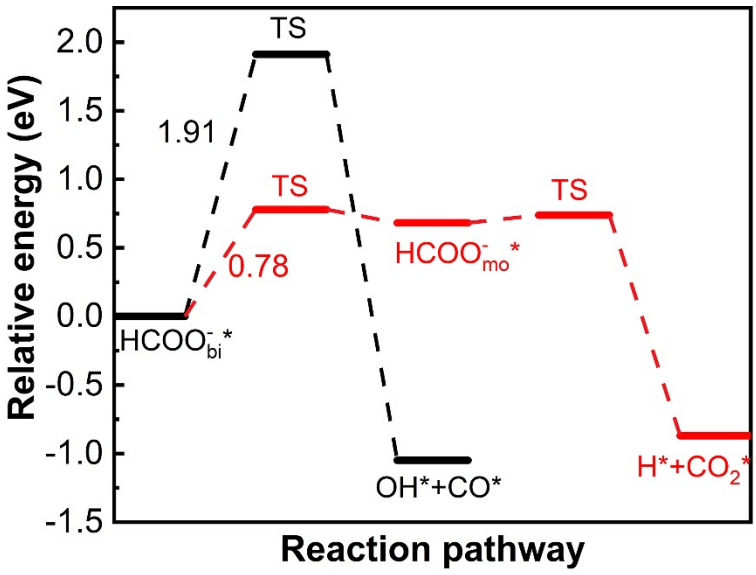

Fig. S12 Kinetic barriers of primary and secondary routes on AgPd-AgF interface for the formate oxidation reaction.

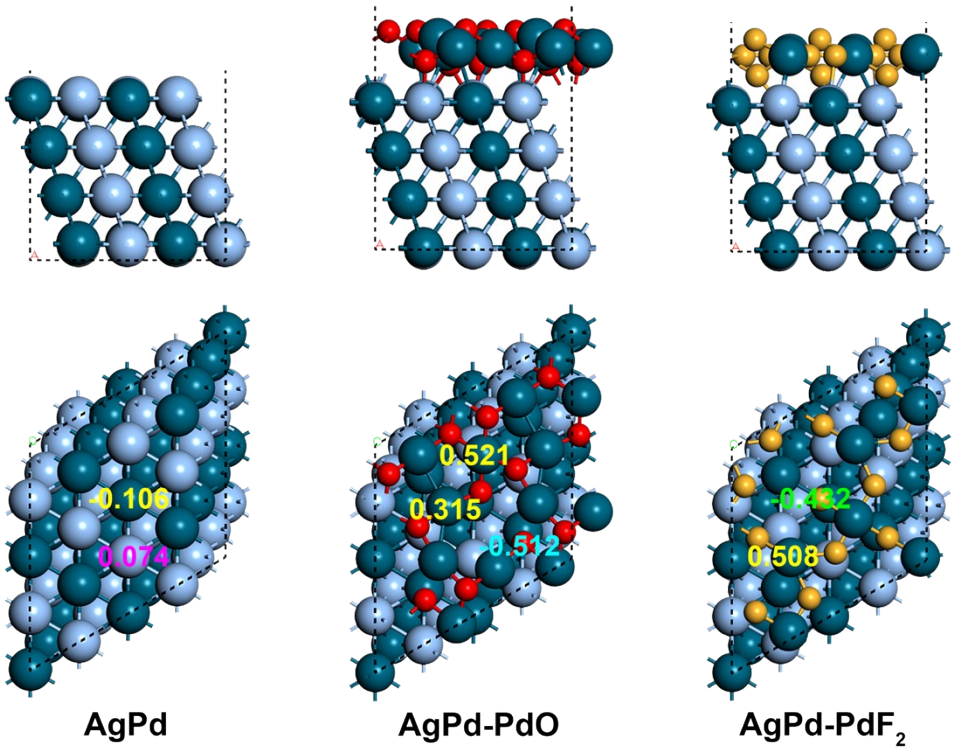

Fig. S13 Front and top view of AgPd-PdO and AgPd-PdF_2 interfaces with refer to AgPd(111) surface, in which the marked number represent the average Mulliken charge.

Table S2. Lattice mismatch (Δ), average interlayer distance between the adlayers and AgPd substrates, and binding energy per metal atom of interfaces between oxide (fluoride) adlayers and AgPd substrates.

System	Δ (%)	d (Å)	E_{bind} (eV atom^{-1})
AgPd	/	2.44	/
AgPd-PdO	8.53%	2.75	-1.37
AgPd-PdF_2	0.74%	2.58	-1.20

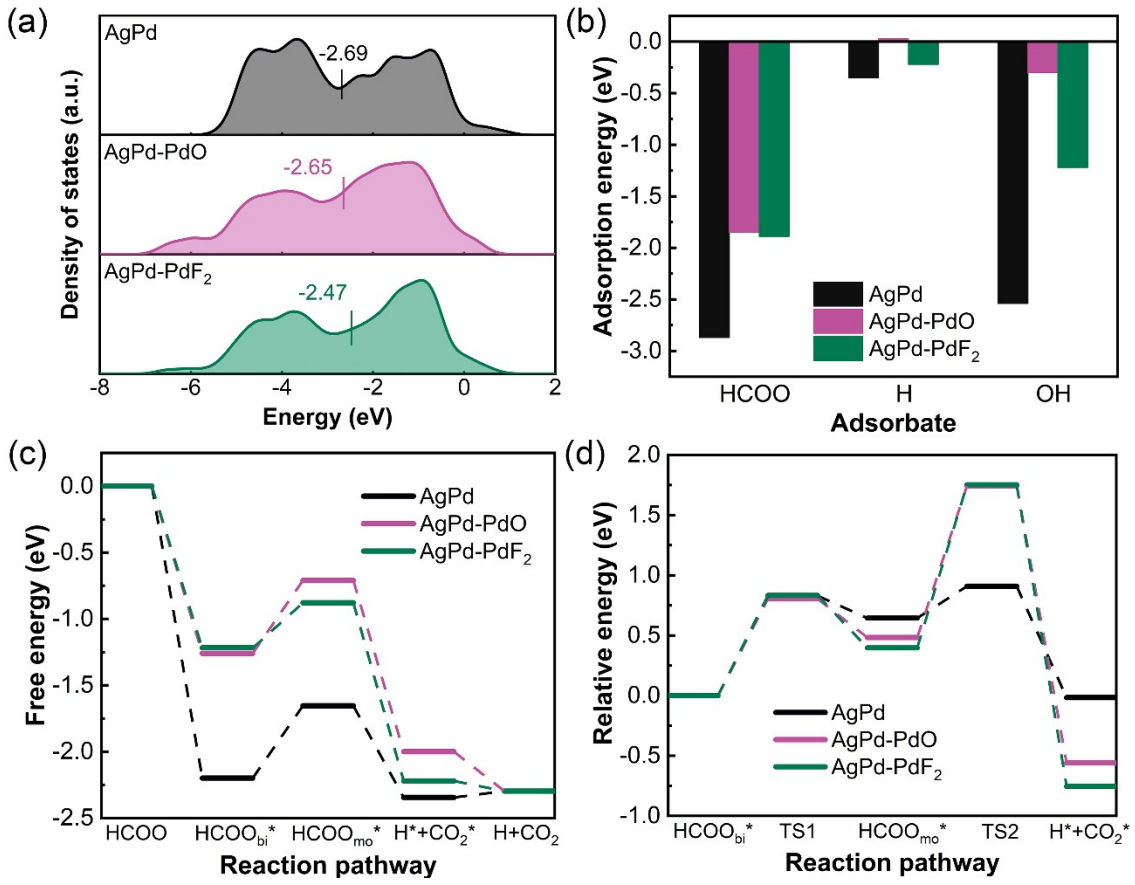

Fig. S14 (a) Partial density of state curves for AgPd-PdO and AgPd-PdF_2 interfaces with refer to AgPd(111) surface, where the vertical line represent the d-band centers. (b-d) Adsorption energies for HCOO, H and OH on the surface of AgPd-PdO and AgPd-PdF_2 interfaces with refer to AgPd(111) surface. (c) Free energy diagram and (d) kinetic barriers on AgPd-PdO and AgPd-PdF_2 interfaces with refer to AgPd(111) surface for the formate oxidation reaction.

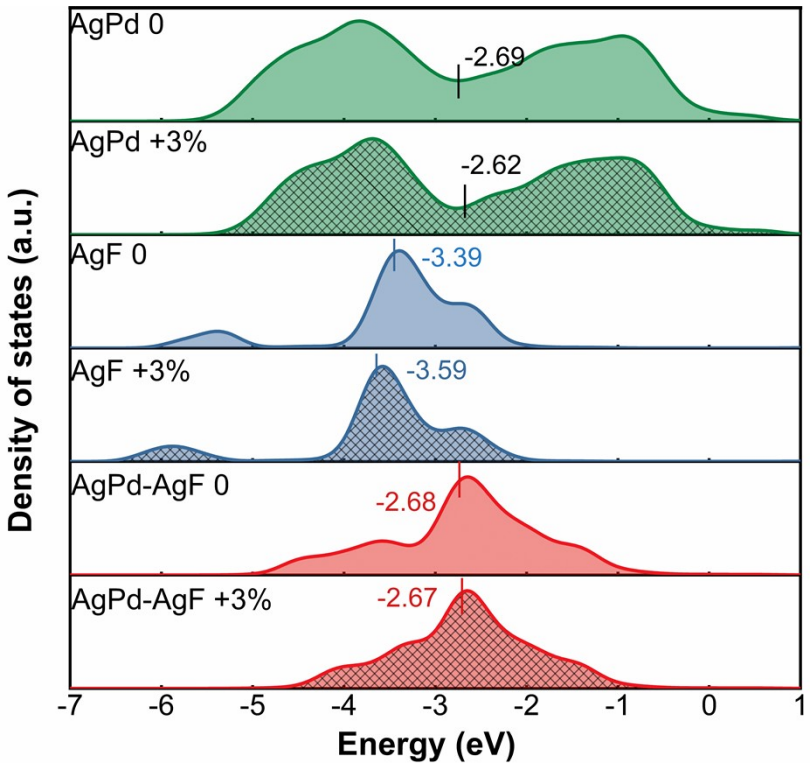

Fig. S15 Partial density of state curves for AgPd, AgF and AgPd-AgF with 0 and 3% of tensile strain, where the vertical line represent the d-band centers.

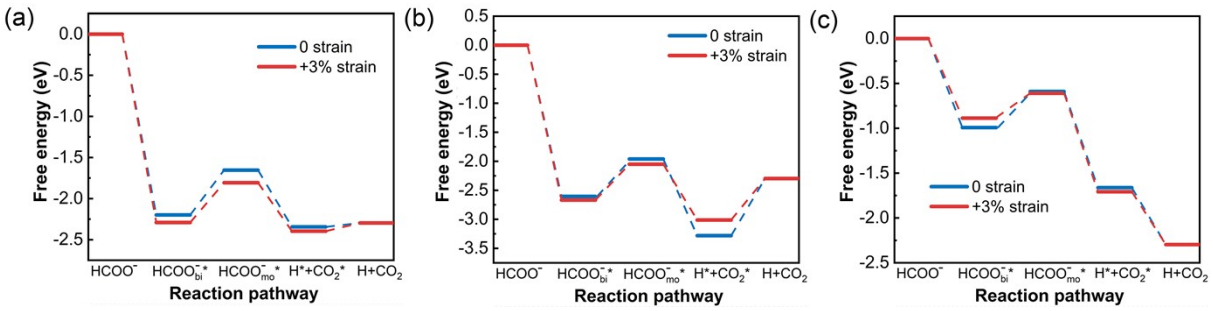

Fig. S16 The Free energy diagram of FOR on the surface of (a) AgPd(111), (b) AgF(111) with 0 and 3% of tensile strain. (c) The Free energy diagram of FOR on the surface of AgF(111) adlayer with 0 and 3% of tensile strain on AgPd(111).

References

1. S. Sankar, G. M. Anilkumar, T. Tamaki and T. Yamaguchi, *ACS Applied Energy Materials*, 2018, **1**, 4140-4149.
2. M. Choun, K. Ham, D. Shin, J. K. Lee and J. Lee, *Catalysis Today*, 2017, **295**, 26-31.
3. S. Roy Chowdhury, S. Ghosh and S. K. Bhattachrya, *Electrochimica Acta*, 2017, **225**, 310-321.
4. J. Noborikawa, J. Lau, J. Ta, S. Hu, L. Scudiero, S. Derakhshan, S. Ha and J. L. Haan, *Electrochimica Acta*, 2014, **137**, 654-660.
5. H. Mao, T. Huang and A. Yu, *International Journal of Hydrogen Energy*, 2016, **41**, 13190-13196.
6. S. Sankar, G. M. Anilkumar, T. Tamaki and T. Yamaguchi, *ChemCatChem*, 2019, **11**, 4731-4737.
7. J. Bai, Q. Xue, Y. Zhao, J.-X. Jiang, J.-H. Zeng, S.-B. Yin and Y. Chen, *ACS Sustainable Chemistry & Engineering*, 2019, **7**, 2830-2836.
8. Q. Tang, F. Chen, T. Jin, L. Guo, Q. Wang and H. Liu, *Journal of Materials Chemistry A*, 2019, **7**, 22996-23007.
9. L. Guo, F. Chen, T. Jin, H. Liu, N. Zhang, Y. Jin, Q. Wang, Q. Tang and B. Pan, *Nanoscale*, 2020, **12**, 3469-3481.
10. Y. Li, Y. He and W. Yang, *Journal of Power Sources*, 2015, **278**, 569-573.
11. Q. Wang, F. Chen, L. Guo, T. Jin, H. Liu, X. Wang, X. Gong and Y. Liu, *Journal of Materials Chemistry A*, 2019, **7**, 16122-16135.
12. B. Pan, F. Chen, B. Kou, J. Wang, Q. Tang, L. Guo, Q. Wang, Z. Li, W. Bian and J. Wang, *Nanoscale*, 2020, **12**, 11659-11671.
13. Q. Tang, F. Chen, Q. Wang, T. Jin, L. Guo, Y. Wu, S. Yu and Z. Li, *Journal of Materials Chemistry A*, 2021, **9**, 23072-23084.
14. Y. Jin, F. Chen, L. Guo, J. Wang, B. Kou, T. Jin and H. Liu, *ACS Applied Materials & Interfaces*, 2020, **12**, 26694-26703.
15. T. T. Gebremariam, F. Chen, B. Kou, L. Guo, B. Pan, Q. Wang, Z. Li and W. Bian, *Electrochimica Acta*, 2020, **354**, 136678.
16. Y. Jin, F. Chen, T. Jin, L. Guo and J. Wang, *Journal of Materials Chemistry A*, 2020, **8**, 25780-25790.
17. J. Wang, F. Chen, Y. Jin, L. Guo, X. Gong, X. Wang and R. L. Johnston, *Nanoscale*, 2019, **11**, 14174-14185.
18. Q. Wang, F. Chen, Q. Tang, L. Guo, T. Jin, B. Pan, J. Wang, Z. Li, B. Kou and W. Bian, *Nano Research*, 2021, **14**, 2268-2276.
19. Q. Wang, F. Chen, Q. Tang, L. Guo, T. T. Gebremariam, T. Jin, H. Liu, B. Kou, Z. Li and W. Bian, *Applied Catalysis B: Environmental*, 2020, **270**, 118861.
20. S.-H. Han, H.-M. Liu, J. Bai, X. L. Tian, B. Y. Xia, J.-H. Zeng, J.-X. Jiang and Y. Chen, *ACS Applied Energy Materials*, 2018, **1**, 1252-1258.
21. S. Sasidharan, A. A. Sasikala Devi, R. Jose, T. Tamaki, A. M. Gopinathan and T. Yamaguchi, *ACS Applied Energy Materials*, 2022, **5**, 266-277.
22. Q.-X. Wang, M.-T. Yuan, H.-Y. Shen, H.-Y. Zhang, X. Chen, Y. Xu, X.-X. Duan, K.-L. Liu, T. Gao, Y.-G. Ning and J. Wang, *Journal of Solid State Electrochemistry*, 2021, **25**, 1197-1205.